

GCN-LSTM: A hybrid graph convolutional network model for schizophrenia classification

Bethany Gosala ^a, Avnish Ramvinay Singh ^a, Himanshu Tiwari ^a, Manjari Gupta ^{a,b,*}

^a DST-Centre for Interdisciplinary Mathematical Sciences, Banaras Hindu University, Varanasi, India

^b Department of Computer Science, Institute of Science, Banaras Hindu University, Varanasi, India

ARTICLE INFO

Keywords:

Electroencephalography (EEG)
Frequency Domain Features (FDF)
Graph Convolutional Networks (GCN's)
Time domain Features (TDF)
Schizophrenia (SZ)
Long short-term memory (LSTM)

ABSTRACT

Schizophrenia is a complex mental disorder that influences one's perceptions, thought processes, social behavior, emotional responses, etc. Electroencephalography is a non-invasive brain imaging technique that measures the brain's electrical activity. The EEG signals are used to study and analyze the human brain. Graphs have always been one of the best ways to represent information. With the inspiration from graphs, in this paper, we developed a novel GCN-LSTM model, a graph-based hybrid deep learning model for classifying schizophrenia from Healthy Control. We used the Institute of Psychiatry and Neurology in Warsaw, Poland dataset to experiment with the developed models; Raw EEG signals were pre-processed and divided into segments of 5-sec and 8-sec. We extracted 14 different features from these epochs, 7 each from the time and frequency domains. After feature extraction, we constructed the graphs out of epochs of 5-sec and 8-sec, where EEG electrodes are considered as nodes and how signal flows between EEG channels as edges. These graphs were fed to the developed GCN-LSTM model for the classification. We also used different seeds and 5-fold cross-validation to avoid overfitting. We conducted several experiments and achieved average accuracy across all seeds as 99.25 ± 0.24 %, Precision of 99.28 ± 0.22 %, F1 score of 99.24 ± 0.24 %, Specificity of 98.73 ± 0.64 ; Sensitivity of 99.67 ± 0.28 and AUC of 99.20 ± 0.27 . We used t-test and one-way ANOVA to study the statistical significance of the extracted features. We found zero crossing rate, mobility (Hjorth parameter), peak frequency, and gamma band.

1. Introduction

As the saying goes, "A healthy mind resides in a healthy body." A general perception about being healthy is being physically fit, ignoring mental health in most cases. Mental health is an essential part of health and well-being that helps individuals cope with the stresses of life. Mental health is crucial to personal, community, and socio-economic development (Mental Health, n.d.).

Mental disorders like depression, anxiety, bipolar disorder, schizophrenia (Sz), Post-Traumatic Stress Disorder (PTSD), etc., will affect the quality of life and influence the cognition, perception, and behavior of an individual [14]. People with severe mental health conditions die 10 to 20 years earlier than the general population. Schizophrenia is one such disorder that affects approximately 24 million people worldwide, it is a chronic and complex mental disorder that primarily impacts individuals' lives and is characterized by a spectrum of cognitive, behavioral, and emotional dysfunctions. Delusions, hallucinations, and

cognitive impairment are the symptoms of schizophrenia; almost 50 % of people in mental hospitals have a schizophrenia diagnosis, and only 31.3 % of people receive specialist mental health care [17].

Neuroimaging techniques are used to study the functionalities of the brain that help in understanding mental disorders; these techniques will help in understanding how the brain works, identifying various brain disorders, finding abnormalities like tumours, etc., [20] Different brain imaging techniques like Electroencephalography (EEG), Magnetoencephalography (MEG), Positron Emission Tomography (PET), Single Photon Emission Computed Tomography (SPECT), Functional Near Infrared Spectroscopy (fNIRS), Computed Tomography (CT), Magnetic Resonance Imaging (MRI) are used to study the brain [8]. EEG is one of the most used non-invasive technique that measure the brain's electrical activity. It is used in both clinical practice and research. EEG has many advantages over other types of neuroimaging techniques; it provides detailed information about the changes that happen due to the brain's electrical activities over time, and it is relatively low cost than other

* Corresponding author.

E-mail address: manjari@bhu.ac.in (M. Gupta).

neuroimaging devices, practical, and portable. Therefore, the use of EEG to diagnose mental illnesses has become one of the popular areas of research. In this area, researchers worked on epilepsy [16], Alzheimer's [25], schizophrenia [6], emotion classification [9], major depressive disorder [4], brain-computer interface (BCI) [1], and studied the influence of Acupuncture efficacy in modelling brain activities [26], etc.

Artificial Intelligence (AI) in healthcare research has seen an enormous jump in the past decade because of the rise of machine learning (ML) and deep learning (DL). Increased computing power with GPUs and TPUs has made these methods work for all types of problems. The use of AI in health care will increase disease classification, prediction, diagnosis, and prognosis [18]. A human brain-inspired neural network (NN), which is the heart of DL, allows computers to process the data and make decisions accordingly. Convolutional neural networks (CNNs) of DL are designed to process grid-like data such as images. CNNs perform tasks like image classification, object detection, image reconstruction, video analysis, and computer vision tasks, etc. [23]. A graph theory-based metric called the SWN index calculates small features from EEG signals by multiplying normalized efficiency with cluster efficiency [28], used in studying the spectral power and functional connectivity of EEG signals by acupuncture stimulation. Functional brain networks were constructed by [27] to extract the network features, and these features were fed as input to a machine learning model for EEG signals from different acupuncture manipulations. Graph Convolutional Networks (GCNs) are the generalized form of CNNs; unlike grids, which are images in CNNs, GCNs have nodes and edges to show the complex structures and relationships among the data. The GCNs are designed in such a way that they can work with irregular data and produce good results in tasks like graph classification, node classification, and link prediction [5].

The main contributions of this work are as follows:

- We have developed two models: a novel 12-layer graph convolutional networks (GCNs) model and a hybrid GCN-LSTM for classifying EEG signals of schizophrenic subjects and healthy control by constructing graphs.
- We extracted 14 different features, seven each from the time and frequency domains, to remove the noise and artifacts and reduce dimensionality. The statistical analysis was done using an independent *t*-test and one-way ANOVA to study the statistical significance among the extracted features.
- Cohesion analysis and phase locking values are calculated using the Hilbert transformation to create edges between the nodes (electrodes) in graphs.
- We experimented with epochs of 5-sec and 8-sec duration on the developed models; our proposed model outperformed all the state-of-the-art models.

This work is organized in the following manner: in section 2, we have given related work; in section 3, a detailed explanation of the methods and methodology that are followed in this work is given. In section 4, an analysis of the obtained results is presented. Section 5 provides the discussion. Finally, we provide conclusions from our study and the future research direction in section 6.

2. Related work

A deep learning-based model for the automatic identification of Schizophrenia (SZ) using EEG data is proposed by [21]. Using Fuzzy means, they have converted EEG signals into a system of radial basis functions, and classification between HC and SZ is done using them. The authors used a dataset that was created at the Psychiatry Department of Virgen de la Luz Hospital in Cuenca (Castilla-La Mancha, Spain); it contains 632 subjects' EEG data, among which 320 are health control (HC) and 312 are schizophrenic. The proposed model is validated using 10-fold cross-validation, and the model is given a balanced accuracy of

93 %, kappa score of 83, and AUC, precision, and recall values of close to 93 % each.

A graph-generative neural networks (GGN) model for epileptic seizure detection using EEG signal via brain functional connectivity is presented in [11]. They used data from Temple University Hospital (TUH) EEG corpus, which contains the Seizure dataset of 3047 epilepsy patient cases, whose sampling frequency is 250 Hz. The developed model is a seven-class classification model and it achieved an accuracy of 91 %.

Lin, P. et al. [12] have conducted a study to analyze how working memory changes in schizophrenia patients when compared with a healthy control group by developing three graph attention network (GAT) based classification models and testing on an open source Zenodo and 0-back task datasets. The first developed model is a simple two-layer GAT model and acquired an accuracy of 77.78 % and 61.10 %; F1 scores of 76.92 % and 44.44 % on Zenodo and 0-back task datasets, respectively. Second is the MGAT model using multiple topologies and multi-functional connections given accuracies of 81.82 %, 71.43 %, F1 scores of 80.00 %, and 74.07 % on the same datasets. The third developed model is MGAT-AIR, an extension of the second model with the adaptive initial residual (AIR) module. This model gave accuracies of 90.90 %, 78.57 %, and F1 scores of 90.90 % and 80.00 % on Zenodo and 0-back task datasets, respectively.

Lin, Z. et al. [13] proposed a hybrid model that combines 1D convolution with graph convolutions to extract the features from intra and inter-channel EEG data for emotion recognition using features extracted from differential entropy and phase lag values. To simulate the relationship between brain regions, the authors used functional connectivity to construct the graph structures. The developed model is validated using 10-fold cross-validation; it achieved average accuracies of 90.74 %, 91 %, and 90.22 % on DEAP-Twente, DEAP-Geneva, and SEED datasets, respectively. Moreover, the model achieved average accuracies of 82.78 %, 84 %, and 83.93 % on the same datasets by using only 20 % of EEG channel data.

The authors [3] conducted a subject-dependent and subject-independent study by building a graph neural network (GNN) model for emotion recognition using EEG signals, standardized low-resolution electromagnetic tomography (sLORETA) method used to map the scalp sensor to brain regions and also as a node for the graphs. Emotion recognition datasets, SEED, and a dataset of the brain-computer interface research lab, University of Tabriz, Iran, are used for the experiments. The proposed model gave an accuracy of 98.75 % in the subject-dependent case and 97.50 % accuracy in the subject-independent case for the developed dataset, and an accuracy of 99.04 %, in the subject-dependent scenario and 98.09 % in subject independent scenario for the SEED database.

An automatic Schizophrenia detection model using graph convolutional neural networks using brain-network features extracted along with time and frequency domain from resting-state electroencephalography (EEG) dataset collected using 59 channel EEG device with 500 Hz sampling frequency. It contains 103 first-episode schizophrenia patients and 92 healthy controls (HC) [24]. Along with five brain frequency bands, they have extracted the Pearson correlation coefficient (PCC), phase-locking value (PLV), and phase-locking index (PLI) from EEG signals and trained the model with varying epoch lengths of 6/8/10 s, also used 10-fold cross-validation model to evaluate the developed model. The best results of 90.01 % accuracy, 88.18 % precision, 94.45 % recall, and 90.85 % F1 score were achieved for theta frequency band with 6 s epoch length and PLV functional connectivity metrics.

GCNs-FSMI, a method that combines fine-grained signals and graph mutual information along with pre-trained graph convolutional neural networks (GCNs) for recognizing mental disorders from EEG signals, is proposed by Li et al. [10]. Before feeding the data to the developed GCNs-FSMI model, they filtered the EEG data channel-wise into six frequency bands, calculated the average power, and combined it with the fine-grained features of the nodes. The developed model is tested on

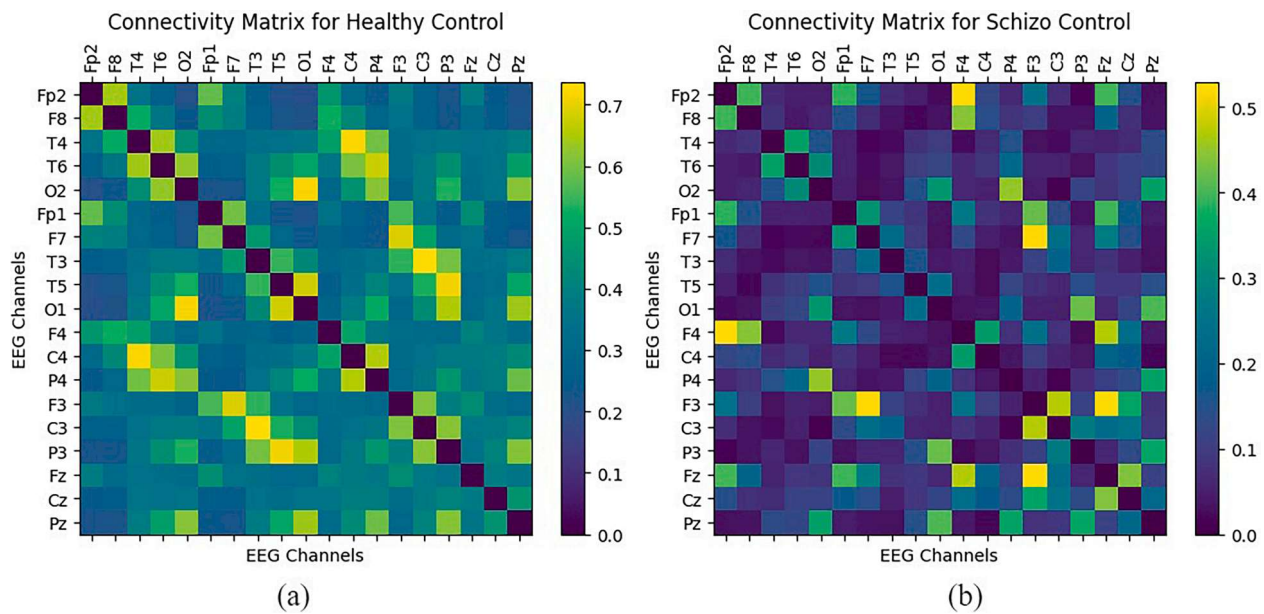


Fig. 1. Coherence plots between each channel of (a) Healthy control (HC) and (b) schizophrenia (SZ) subjects.

the IEEE Healthcom 2020/MODMA dataset, which contains resting-state EEG data of depressive disorder and SCHIZ data set from the Laboratory for Neurophysiology and Neuro-Computer Interfaces of Moscow State University. The GCNs-FSMI model achieved the best accuracy of 97.18 on the MODAM dataset and 78.17 on the SCHIZ dataset.

A novel graph convolutional network model, a combination of convolutional neural networks with brain topology graph embedding for motor imagery EEG signal classification, is presented in [19]. This model extracted spatiotemporal features by convolutional blocks using depth-wise convolutions, while temporal features were extracted using a temporal convolutional network (TCN). It achieved 80.46 % and 94.38 % accuracy on BCICIV-2a and HGD datasets, respectively.

The authors [6] have conducted a study on three different wavelet transforms which are continuous wavelet transform (CWT), discrete wavelet transform (DWT), and wavelet scattering transform (WST), by extracting 12 statistical features from data before feeding the data to various machine learning models. The authors used an EEG dataset containing 14 healthy controls and 14 schizophrenia subjects' data developed at the Institute of Psychiatry and Neurology in Warsaw, Poland. Overall best results were achieved by the support vector model (SVM), with an accuracy of 97.98 %, sensitivity of 98.2 %, specificity of 97.72 %, and kappa score of 95.94 %.

3. Methodology

3.1. Dataset

The dataset used in this work is collected at the Institute of Psychiatry and Neurology in Warsaw, Poland [15], it contains EEG signal data from 28 subjects of which 14 are healthy controls and 14 have paranoid schizophrenia, and these signal are collected using a 19 channel EEG device, with a sampling frequency of 250 Hz using the standard 10–20 EEG montage. Since the healthy control and diseased signal data have an equal number of samples the dataset is balanced, but the duration of both is different which creates a difference in epochs created. The entire dataset contains more than 8 h of EEG signal, in which healthy control signal duration is about 3 h 37 min and the schizophrenic signal is about 4 h and 25 min, on an average 15 min signal is collected from each HC and 18 min signal is collected from each SZ. We have calculated the coherence of health control and schizophrenic signals, it gives the degree of linear dependency of two signals in terms of similar frequency

components, shown in Fig. 1. We have illustrated the coherence between each channel of HC and SZ.

3.2. Preprocessing

The raw EEG signal was read using the Python MNE library, and bandpass filtering was applied to the raw signal to remove the high-frequency noise and artifacts; pass-band and stop-band values were set to 0.5 Hz and 50 Hz, respectively, also using a standard 10–20 montage system along with average referencing. Then we segmented the data into 5-sec and 8-sec length signals with 1-sec of overlap on each segment and created epochs out of these segments; a total of 7201 epochs were created for 5-sec epoch duration, and 4108 epochs were created for 8-sec epoch duration. After creating epochs, we have extracted 14 features from each epoch, 7 time domain features, and 7 frequency domain features. The extracted features from each subject are saved as separate parquets, creating 28 parquet files of 28 subjects; these parquets can directly feed to the developed model.

3.3. Feature extraction

3.3.1. Time domain features

Time-domain features (TDFs) are statistical and signal-processing measures that can be extracted directly from raw signals. TDFs capture a signal's morphological characteristics over time. We have extracted 7 TDFs from EEG signals, which are discussed below.

Mean: Mean provides the central tendency of the signal, it gives the average value of amplitude over a specified window of duration given by Eq. (1),

$$\text{Mean} = \frac{1}{N} \sum_{i=1}^N x_i \quad (1)$$

Where x_i is the amplitude of the EEG signal at a given time i

N is the total number of samples.

Variance: Variance is a measure that talks about the spread of the EEG signal amplitude around the mean. If fluctuations in the signal are more, then the variance value will be high, it is calculated using Eq. (2),

$$\text{Variance} = \frac{1}{N} \sum_{i=1}^N (x_i - \text{Mean})^2 \quad (2)$$

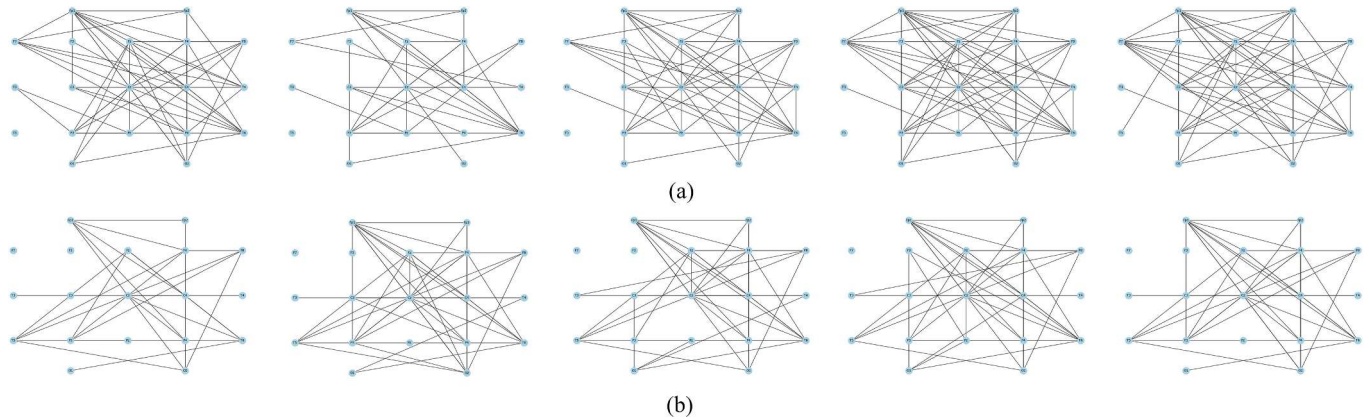
Standard deviation: It is the square root of the variance, which

Table 1

Statistical analysis of extracted features using t-test and one-way ANOVA.

Feature	T-Test Analysis				One-way ANOVA Analysis			
	5-sec epochs signal		8-sec epochs signal		5-sec epochs signal		8-sec epochs signal	
	t_value	p_value	t_value	p_value	f_value	p_value	f_value	p_value
f1	0	0.5	0	0.5	1.08E-32	1	7.91E-32	1
f2	-21.607	1.88E-12	-18.583	1.45E-11	13.7683	0.0009	14.3239	0.0008
f3	-21.578	1.92E-12	18.562	1.47E-11	13.8440	0.0009	14.3762	0.0008
f4	-71.24	1.25E-19	-54.585	5.14E-18	104.9357	1.28E-10	112.0426	6.41E-11
f5	-3.875	0.0008	-3.991	0.0006	3.4570	0.0743	3.4652	0.0740
f6	-58.18	2.11E-18	-43.421	1.24E-16	67.4224	1.08E-08	65.7072	1.38E-08
f7	1.757	0.0503	0.928	0.1845	22.5312	6.56E-05	21.0713	9.91E-05
f8	38.238	6.66E-16	28.859	3.55E-14	21.2538	9.41E-05	21.0589	9.95E-05
f9	-72.251	1.03E-19	-54.921	4.71E-18	52.5884	1.06E-07	55.6911	6.35E-08
f10	24.389	3.60E-13	18.257	1.84E-11	32.6316	5.19E-06	34.9891	3.06E-06
f11	29.181	3.05E-14	22.446	1.12E-12	22.2452	7.10E-05	26.2647	2.42E-05
f12	2.069	0.0287	1.638	0.0618	46.2290	3.24E-07	47.5634	2.54E-07
f13	18.071	2.12E-11	15.079	2.37E-10	22.5296	6.56E-05	23.4321	5.12E-05
f14	-63.063	6.86E-19	-47.256	3.83E-17	44.6347	4.35E-07	43.4721	5.42E-07

*f1 = mean, f2 = standard deviation, f3 = Root mean square (RMS), f4 = Zero crossing rate (ZCR), f5 = activity, f6 = mobility, f7 = complexity, f8 = spectral entropy, f9 = peak frequency, f10 = delta band, f11 = theta band, f12 = alpha, f13 = beta band, f14 = gamma band.

**Fig. 2.** EEG signal graphs plots of 5 epochs of (a) schizophrenia, (b) healthy control.

provides the dispersion of the EEG signal and is given by Eq. (3),

$$\text{Standard deviation} = \sqrt{\text{Variance}} \quad (3)$$

Root mean square (RMS): It is a reflection of the signal's power, RMS of the EEG signal represents the square root of the average of the squared signal amplitudes. It is calculated using Eq. (4),

$$\text{RMS} = \sqrt{\frac{1}{N} \sum_{i=1}^N x_i^2} \quad (4)$$

Zero crossing rate (ZCR): Zero crossing rate (ZCR) is a rate at which the EEG signal changes sign i.e., crossing the zero amplitude line. In other words, it gives the oscillatory nature of the EEG signal, an implementation of zero-crossing for a signal x_i at a window k is given as Eq. (5)

$$\text{ZCR}_k = \sum_{h=kM}^{kM+N} |\text{sign}(x_h) - \text{sign}(x_{h-1})| \quad (5)$$

Where M is the step between the analysis window and N is the analysis window length

Hjorth Parameters: Hjorth parameters are obtained using signal processing techniques in the time domain, there are three Hjorth parameters: activity, mobility, and complexity.

Activity: Activity gives the squared standard deviation of the amplitude of the signal which indicates the surface of the power spectrum in the frequency domain, i.e., activity value is less if the lower frequency components are more common, and high otherwise. Activity

corresponds to the variance of the signal.

Mobility: Mobility of EEG signal is the proportion of standard deviation of the power spectrum or the mean frequency. It is the square root of the activity of the first derivative of the signal divided by the activity of the signal and is given as Eq. (6)

$$\text{Mobility} = \sqrt{\frac{\text{Variance of } \frac{dx}{dt}}{\text{Variance of } x}} \quad (6)$$

Complexity: Complexity estimates the signal's bandwidth and indicates how the signal's shape is similar to the pure sine wave. In other words, it is the ratio of mobility of the first derivative of the signal to the mobility of the signal and is given below Eq. (7)

$$\text{Complexity} = \frac{\text{Mobility of } \frac{dx}{dt}}{\text{Mobility of } x} \quad (7)$$

3.3.2. Frequency domain features

The time domain signals can be viewed in the frequency domain by applying mathematical transforms like fast Fourier transform (FFT) and Welch's method and features like power spectrum density, entropy, wavelet transforms, etc., can be extracted from the frequency domain. In this work, frequency domain analysis is done by extracting the power spectrum density of the EEG signal using Welch's method, and then we extracted 7 frequency domain features from the signal.

Brain wave frequencies: we have extracted five brain frequency features from the EEG signal after applying Welch's method, which is

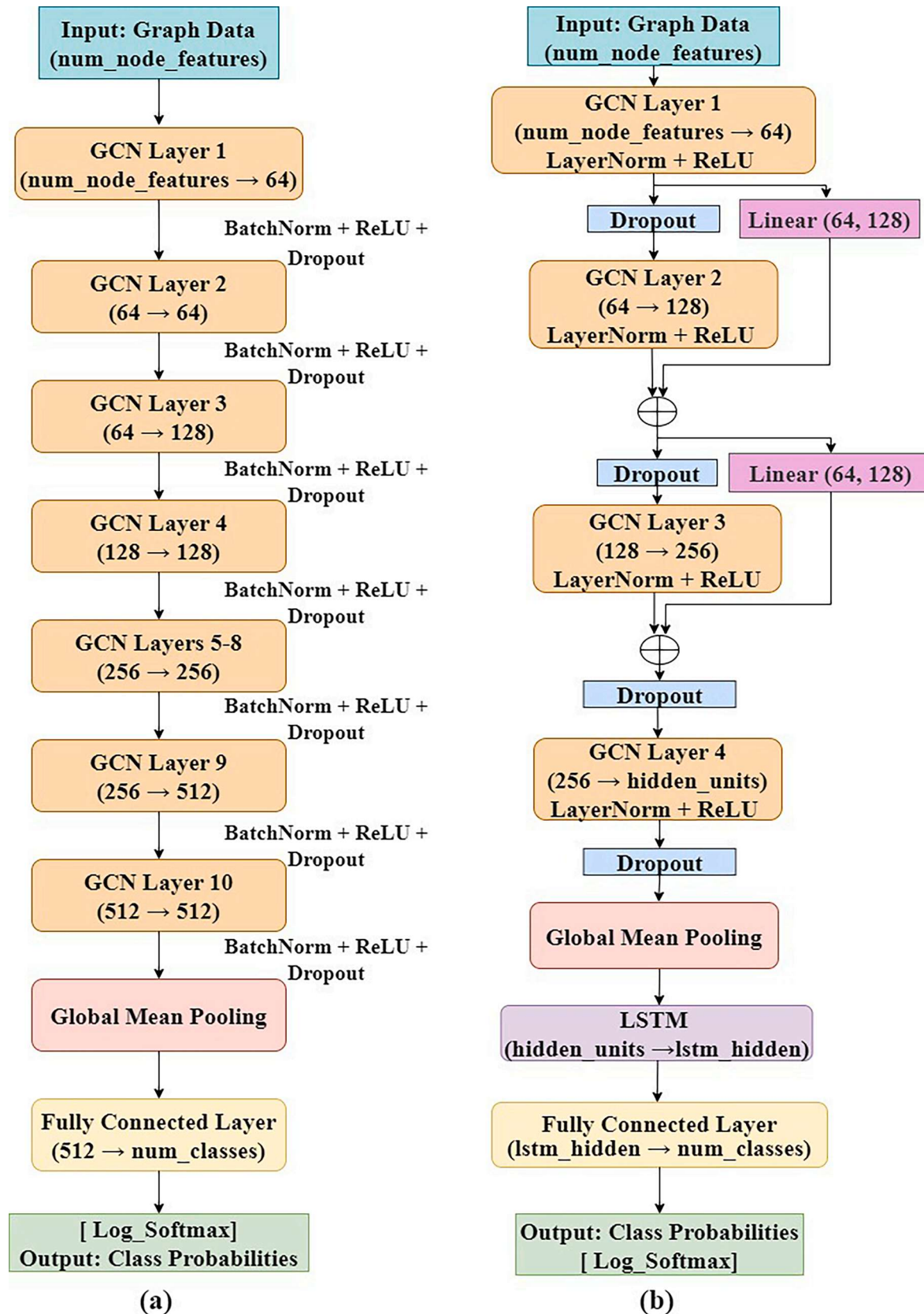


Fig. 3. (a) Model_1: An 12 layer GCN model (b) Model_2: A hybrid GCN_LSTM model.

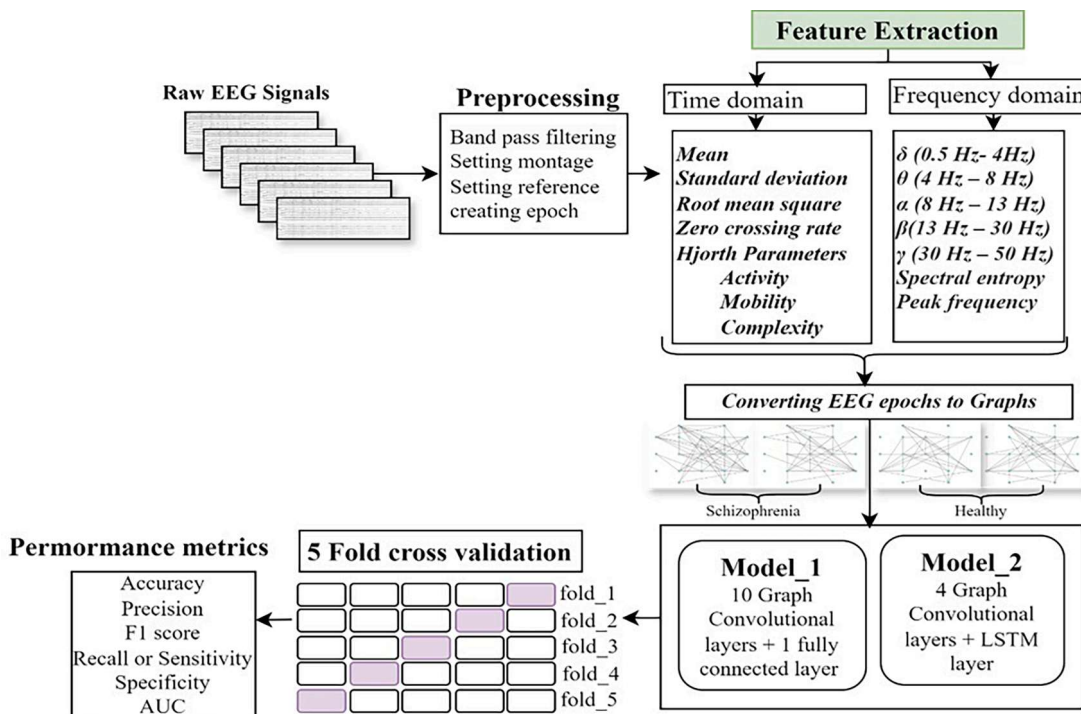


Fig. 4. Experimental flow diagram.

	Actually Positive (1)	Actually Negative (0)
Predicted Positive (1)	True Positives (TPs)	False Positives (FPs)
Predicted Negative (0)	False Negatives (FNs)	True Negatives (TNs)

Fig. 5. Confusion Matrix.

the delta (δ) (0.5 Hz- 4 Hz), theta (θ) (4 Hz – 8 Hz) alpha (α) (8 Hz–13 Hz) beta (β) (13 Hz–30 Hz) gamma (γ) (30 Hz – 50 Hz).

Spectral entropy: It measures the randomness or complexity of the EEG signal by quantifying the distributions of power across different frequency bands. It is defined to be the Shannon Entropy of the power spectral density (PSD) of EEG data and is given by Eq. (8)

$$H = - \sum_{i=1}^N P(f_i) \log[P(f_i)] \quad (8)$$

Where $P(f_i)$ is the normalized power at frequency f_i and N is the number of frequency bins.

Peak frequency: It is the frequency at which the power spectrum density (PSD) attains maximum value. The “argmax()” function is commonly used in this context to identify the index of the maximum value in the PSD array.

3.4. Statistical significance between the extracted features

We performed statistical analysis on 14 extracted features, we analyzed the features using two statistical analysis techniques which are t-test and One-way ANOVA. Both t-test and one-way ANOVA are used to

compare the means between the groups, we used the independent t-test function `ttest_ind()` and considered $p < 0.05$, and `f_oneway()` function from `sciPy` package for the analysis along with R software for finding the *t-value*, *f_value*, and *p_value* these are shown in Table. 1. In ANOVA analysis for $df1 = 1$ (degree of freedom between groups) in our case, $k = 2$, i.e., number of groups (healthy, schizophrenic) and $df1 = k - 1$, and $df2 = 26$, since we have 14 feature form each group and we have two groups (14x2) therefore $n = 28$, and $df2 = n - k$ (degree of freedom within groups).

From the above Table. 1., we can observe that zero crossing rate (ZCR) (f4), mobility (f6), peak frequency (f9), and gamma band (f14) are the top four highly significant features (highlighted in bold font) according to both t-test and one-way ANOVA analysis. Mean (f1), Hjorth Parameters' activity (f5), Hjorth Parameters' complexity (f7), and alpha band (f12) are the top four least significant features (highlighted in italics) according to t-test analysis and mean (f1), standard deviation (f2), root mean square (RMS) (f3), and activity (f5) are the least significant features (highlighted in italics) according to one-way ANOVA analysis. Mean (f1) is the least significant feature, according to t-test and one-way ANOVA. This might be because both t-test and one-way ANOVA use means between the groups to compare, and the feature itself is a mean. Hence, this feature gets nullified when these tests are applied on it.

3.5. Graph convolutional networks (GCNs)

A generalization of traditional neural networks to graph-structured data can be possible through graph neural networks (GNNs). GNNs work on networked data, like graphs, by learning from the structures and relationships present in the graphs. Graph neural networks are particularly useful in applications that generate data from non-Euclidean domains and represent graphs with complex relationships. Mainly, GNNs are divided into 4 categories: convolutional graph neural networks, recurrent graph neural networks, spatial-temporal graph neural networks, and graph autoencoders [2,22]. We used graph convolutional neural networks (GCNs) to build the graphs from EEG signals, as graphs have nodes and edges; in GCNs, we have considered EEG

Table 2

Performance metrics of GCN_5 model for various seeds.

Performance Metrics		Accuracy	Precision	F1 Score	Specificity	Sensitivity	AUC
seed = 42	fold_1	77.21	77.16	77.11	74.64	79.51	77.08
	fold_2	83.30	84.28	83.00	73.97	91.69	82.83
	fold_3	79.57	80.49	79.53	88.38	71.65	80.01
	fold_4	84.16	84.42	84.16	89.02	79.80	84.41
	fold_5	83.05	83.01	83.03	83.86	82.33	83.09
seed = 52	fold_1	79.36	80.21	79.33	87.85	71.73	79.79
	fold_2	75.23	76.67	75.12	86.56	65.06	75.81
	fold_3	81.90	82.83	81.87	90.69	74.04	82.35
	fold_4	79.36	79.45	79.21	74.88	83.39	79.13
	fold_5	78.83	81.90	78.89	63.79	92.54	78.72
seed = 62	fold_1	86.30	86.44	86.21	82.68	89.55	86.12
	fold_2	79.96	80.77	79.93	88.26	72.50	80.38
	fold_3	75.73	75.76	75.57	71.33	79.69	75.51
	fold_4	83.11	83.32	82.96	78.11	87.60	82.85
	fold_5	79.48	80.04	79.47	86.38	73.29	79.83
seed = 72	fold_1	76.68	77.48	76.65	84.97	69.23	77.10
	fold_2	82.15	82.51	82.15	87.79	77.08	82.44
	fold_3	81.33	81.35	81.32	83.39	79.48	81.44
	fold_4	81.86	81.95	81.86	85.06	78.98	82.02
	fold_5	80.47	80.52	80.46	83.01	78.19	80.60
seed = 82	fold_1	82.39	82.97	82.38	89.40	76.08	82.74
	fold_2	71.55	72.06	71.54	78.19	65.59	71.89
	fold_3	86.29	86.47	86.19	82.21	89.95	86.08
	fold_4	81.28	82.16	81.25	89.90	73.53	81.71
	fold_5	85.43	85.73	85.43	90.69	80.70	85.69

Table 3

Performance metrics of GCN_8 model for various seeds.

Performance Metrics		Accuracy	Precision	F1 Score	Specificity	Sensitivity	AUC
seed = 42	fold_1	83.93	86.03	83.20	69.92	95.43	82.67
	fold_2	87.77	88.60	87.45	79.53	94.54	87.04
	fold_3	91.35	91.39	91.24	88.87	93.39	91.13
	fold_4	90.33	90.61	90.16	85.69	94.14	98.92
	fold_5	90.55	90.67	90.41	87.09	93.39	90.24
seed = 52	fold_1	90.67	91.71	91.56	89.25	93.66	91.45
	fold_2	83.78	85.42	83.13	71.12	94.19	82.65
	fold_3	92.67	92.88	92.56	89.14	95.56	92.35
	fold_4	84.78	84.61	84.46	85.25	84.39	84.82
	fold_5	91.96	92.11	91.84	88.66	94.68	91.67
seed = 62	fold_1	91.18	91.27	91.06	88.17	93.66	90.91
	fold_2	83.98	84.20	83.66	77.69	89.14	83.41
	fold_3	89.67	90.57	89.40	81.74	96.18	88.96
	fold_4	92.30	92.33	92.21	90.22	94.05	92.12
	fold_5	91.28	91.19	91.20	90.44	91.97	91.20
seed = 72	fold_1	86.02	86.84	85.64	77.21	93.26	85.23
	fold_2	91.94	92.09	91.82	88.66	94.63	91.64
	fold_3	91.69	91.82	91.58	88.55	94.28	91.41
	fold_4	90.01	90.17	89.86	86.12	93.21	89.67
	fold_5	92.33	92.22	92.26	92.17	92.46	92.31
seed = 82	fold_1	80.35	83.23	79.17	62.74	98.81	78.77
	fold_2	89.97	89.88	89.86	88.66	91.04	89.85
	fold_3	91.50	91.36	91.43	91.84	91.22	91.53
	fold_4	90.11	90.59	89.91	84.23	94.94	89.59
	fold_5	82.44	84.60	81.60	67.65	94.59	81.12

electrodes from which data is collected as nodes and the connections between the electrodes as edges. The layer-wise propagation rule for a GCN can be represented as Eq. (9)

$$H^{l+1} = \sigma \left(\hat{D}^{-\frac{1}{2}} \hat{A} \hat{D}^{-\frac{1}{2}} H^l W^l \right) \quad (9)$$

Where \hat{A} is the adjacency matrix with added self-loops.

\hat{D} is the degree matrix of \hat{A} .

H^l is the node feature matrix at layer l .

W^l is the learnable weight matrix at layer l .

σ is an activation function

Functional connectivity metrics are used to construct the brain

networks that are used to obtain graph structures, and these graphs are fed as input to GCNs. Previous studies have mainly used functional connectivity metrics like Pearson correlation coefficient (PCC), phase-locking value (PLV), and phase-lag index (PLI), etc., [24]. In our work, we have used phase-locking value (PLV) and coherence, which were not used together in previous studies, as functional connectivity metrics to construct brain networks. Coherence analysis was performed to assess the synchronicity of brain activity across different areas, revealing patterns of neural connectivity. For each EEG signal, coherence matrices were constructed, illustrating the connectivity landscape of the brain. In parallel, the Phase Locking Value (PLV) was calculated to examine the synchronization between pairs of brain regions, using instantaneous phase information derived from the Hilbert transform. This provided a detailed view of the phase relationship consistency across signals,

Table 4

Performance metrics of GCN_LSTM_5 model for various seeds.

Performance Metrics		Accuracy	Precision	F1 Score	Specificity	Sensitivity	AUC
seed = 42	flop_1	98.73	98.79	98.73	97.68	99.68	98.68
	flop_2	98.76	98.79	98.75	98.06	99.39	98.72
	flop_3	98.63	98.61	98.63	98.97	98.33	98.65
	flop_4	98.58	98.55	98.58	99.09	98.12	98.60
	flop_5	97.70	97.68	97.70	99.67	95.93	97.80
seed = 52	flop_1	98.70	98.68	98.70	99.06	98.39	98.72
	flop_2	98.50	98.46	98.49	99.23	97.83	98.53
	flop_3	98.38	98.41	98.38	97.82	98.89	98.36
	flop_4	98.52	98.50	98.52	98.88	98.20	98.54
	flop_5	96.62	96.66	96.62	99.88	93.69	96.79
seed = 62	flop_1	98.48	98.45	98.48	99.00	98.02	98.51
	flop_2	97.73	97.69	97.73	98.73	96.83	97.78
	flop_3	98.79	98.79	98.78	98.59	98.97	98.78
	flop_4	98.72	98.73	98.71	98.29	99.10	98.70
	flop_5	98.56	98.57	98.56	98.32	98.78	98.55
seed = 72	flop_1	96.86	97.13	96.84	93.72	99.68	96.70
	flop_2	99.06	99.07	99.06	98.79	99.31	99.05
	flop_3	98.27	98.27	98.27	98.12	98.41	98.27
	flop_4	98.70	98.67	98.70	99.55	97.94	98.75
	flop_5	98.91	98.87	98.91	99.32	98.54	98.93
seed = 82	flop_1	98.81	98.88	98.81	97.76	99.76	98.76
	flop_2	98.59	98.60	98.59	98.35	98.81	98.58
	flop_3	98.45	98.55	98.45	96.97	99.78	98.38
	flop_4	98.45	98.46	98.45	98.23	98.65	98.44
	flop_5	99.01	99.02	99.01	98.62	99.36	98.99

Table 5

Performance metrics of GCN_LSTM_8 model for various seeds.

Performance Metrics		Accuracy	Precision	F1 Score	Specificity	Sensitivity	AUC
seed = 42	flop_1	99.00	98.94	98.99	99.46	98.62	99.04
	flop_2	99.46	99.51	99.45	98.86	99.95	99.41
	flop_3	99.48	99.49	99.48	99.29	99.64	99.47
	flop_4	99.39	99.44	99.38	98.75	99.91	99.33
	flop_5	98.80	98.91	98.79	97.51	99.86	98.69
seed = 52	flop_1	99.41	99.41	99.41	99.29	99.51	99.40
	flop_2	94.83	95.70	94.72	88.55	100.00	94.27
	flop_3	98.68	98.77	98.67	97.51	99.64	98.58
	flop_4	99.48	99.46	99.48	99.67	99.33	99.50
	flop_5	98.85	98.85	98.84	98.59	99.06	98.83
seed = 62	flop_1	98.78	98.70	98.77	99.67	98.04	98.86
	flop_2	98.61	98.74	98.59	97.08	99.86	98.47
	flop_3	98.90	98.92	98.89	98.48	99.24	98.86
	flop_4	99.41	99.45	99.40	98.92	99.82	99.37
	flop_5	96.88	97.24	96.83	93.46	99.68	96.57
seed = 72	flop_1	99.46	99.46	99.45	99.29	99.6	99.44
	flop_2	99.58	99.58	99.58	99.46	99.68	99.57
	flop_3	98.70	98.82	98.69	97.35	99.82	98.58
	flop_4	98.95	98.98	98.94	98.38	99.42	98.9
	flop_5	98.05	98.24	98.02	95.95	99.77	97.86
seed = 82	flop_1	99.09	99.12	99.08	98.65	99.46	99.05
	flop_2	99.46	99.44	99.45	99.51	99.42	99.46
	flop_3	99.26	99.27	99.26	99.02	99.46	99.24
	flop_4	99.02	99.11	99.01	97.94	99.91	98.92
	flop_5	99.53	99.52	99.53	99.56	99.51	99.54

enhancing our understanding of the brain's network dynamics in schizophrenia. Coherence and Phase Locking Value (PLV) can be calculated using the formula given in Eqs. (10) & (11), respectively.

Coherence: Given two signals $x(t)$ and $y(t)$, their coherence $C_{xy}(f)$ at frequency f is defined as Eq. (10):

$$C_{xy}(f) = \frac{|S_{xy}(f)|^2}{S_{xx}(f)S_{yy}(f)} \quad (10)$$

Where $S_{xy}(f)$ is the cross-spectral density (CSD) between $x(t)$ and $y(t)$.

$S_{xx}(f), S_{yy}(f)$ are the power spectral densities (PSDs) of $x(t)$ and $y(t)$, respectively.

Phase Locking Value (PLV): Given two signals $x(t)$ and $y(t)$, their

instantaneous phases $\phi_x(t)$ and $\phi_y(t)$ can be obtained using the Hilbert transform. The PLV is calculated using the given Eq. (11),

$$PLV = \left| \frac{1}{N} \sum_{t=1}^N e^{j(\phi_x(t) - \phi_y(t))} \right| \quad (11)$$

Where N is the number of time points.

j is the imaginary unit.

Graph Construction

We have used networkx [7], a Python software package to build the graphs for each created epoch. It is used to manipulate, create, and also to study the dynamics, structure, and functions of complex networks. It helps in understanding the data that is represented as massive complex networks in the form of graphs with nodes and edges. The EEG dataset

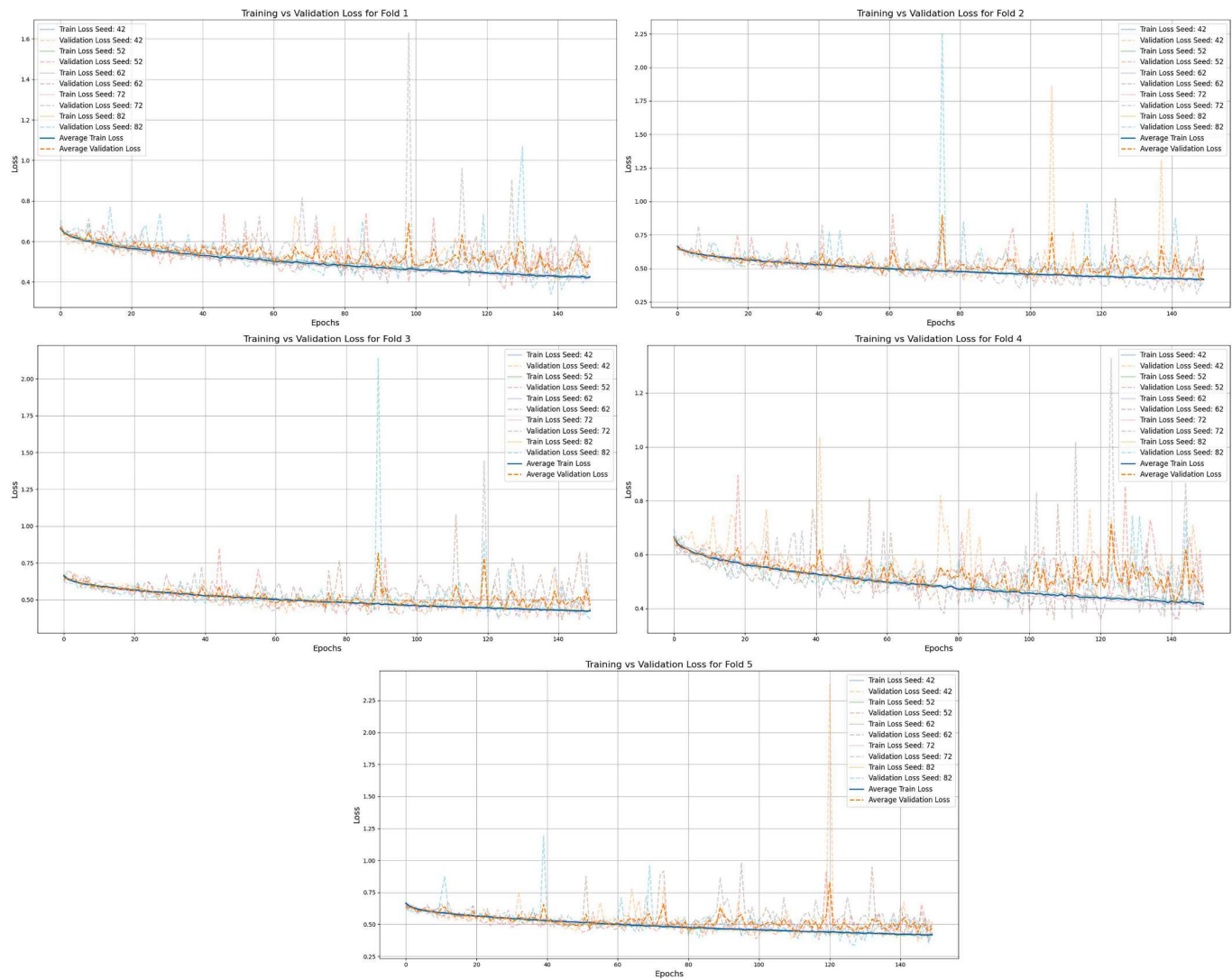


Fig. 6. The Loss function plot varying across five folds for different seeds for the GCN_5 model.

we used in this work is collected from a 19-channel EEG device. So, the graphs we constructed have 19 nodes corresponding to the number of electrodes from which the data is collected and the relation between the electrodes as edges. The constructed graphs for an epoch are shown in Fig. 2.

Graph-based feature extraction representation of EEG has several advantages over traditional time-domain, frequency-domain, and periodic and aperiodic Power Spectral Density (PSD) parameters. Graph-based representation captures structural and Functional connectivity from the EEG signal. Graph-based features are very good at capturing inter-channel connectivity; which plays a vital role in schizophrenia classification. It also reveals the signal's higher-order relationships, topological structures, and network dynamics that are not provided by traditional features. Graphs are robust to noise and track the dynamic changes in the brain networks, making them ideal for complex brain activity features.

3.6. Experimental Design

In our experiments, we divided the dataset into an 80:20 ratio, where 80 % of the data was used for training the model. We built two models based on GCNs and conducted several experiments by trying different hyperparameters. The values for which the best results were obtained are presented below.

3.6.1. Model 1

A GCN model contains 10 graph convolutional layer model followed by batch normalization layers, then a global mean pooling layer and fully connected layer and at softmax for classification. A brief explanation of each layer used to build model_1 is discussed below

Input layer: It is the first layer of the model where we feed the graphs (graph structure and node features) into the neural network before any graph convolution happens. Unlike in CNNs or MLPs, there is no separate “input transform” at this stage—any transformations start in the first GCN layer. Data passing and dimension alignment are also done through the input layer only.

Graph convolutional layers (GCN): A GCN layer handles the graph data and generalizes the 2D convolution from images (pixels having grid like structure) to graphs (having an irregular structure of nodes and edges). Each node in the graph collects the information from its neighbouring node; after aggregation, normalization, linear transform and nonlinearity will be done. GCN layers are good at leveraging graph structures, parameters efficiency, local to global reasoning, etc.,

BatchNorm: Batch Normalization normalizes each feature channel by subtracting the batch mean and dividing by the batch standard deviation. It helps the network experience more stable gradients and can often train faster. It also keeps the activation function from drifting too much across training and improves generalization.

ReLU: ReLU is an activation function, it zeros all negative values by

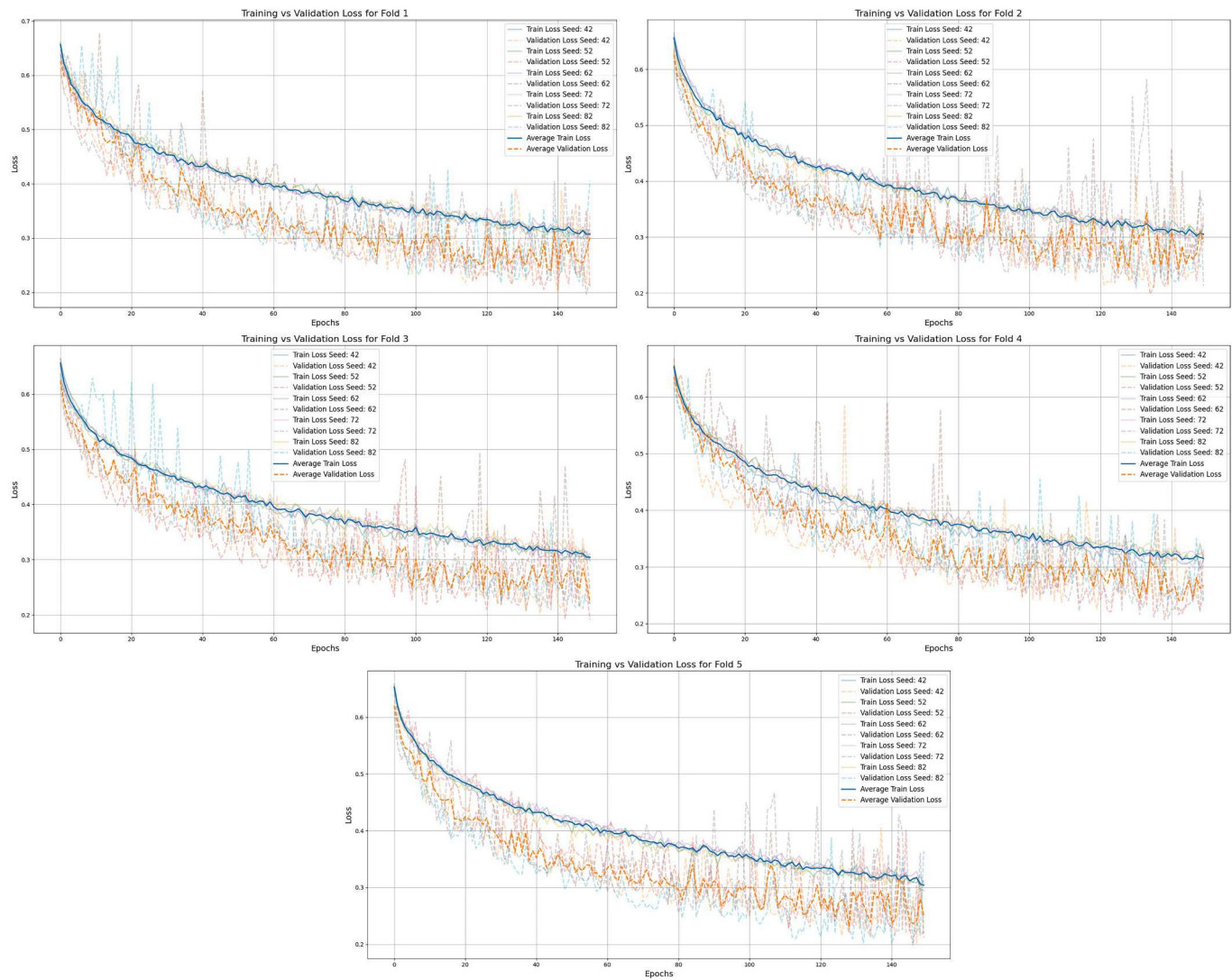


Fig. 7. The Loss function plot varying across five folds for different seeds for the GCN_8 model.

leaving positive values unchanged. It does computation efficiently, and reduces the vanishing gradient problem, and reduces sparsity.

Dropout: Dropout randomly sets a fraction of the neurons' outputs to zero during training. It prevents overfitting by forcing the network not to rely too heavily on any single neuron or path of neurons.

Global mean pooling: Global mean pooling is an aggregation operation that reduces a set of feature vectors into a single average vector. In GCNs, global mean pooling transforms multiple features from multiple nodes into a single, fixed-sized representation. It is easy to implement, reduces parameters, handles data of variable sizes, and is order invariant.

Fully connected: The fully connected (FC) layer, or a dense layer, is one of the fundamental layers of the neural network. It takes the input vector and multiplies it by a weight matrix, then adds a bias and applies a nonlinearity. It combines all the extracted features to perform classification or regression. We used softmax for the final classification.

The number of layers, along with the type and the sequence in which they are used, are shown in Fig. 3(a). The hyper-parameters used in this model_1 are batch_size = 32, random_state = 42, 52, 62, 72, 82, learning_rate = 0.0001, activation_function = ReLU, dropout = 0.08.

3.6.2. Model_2

A hybrid GCN-LSTM model with 4 graph convolutional layers along with 4 layer norms, two transform layers to match the dimensions after

the first and second GCN layers then followed by an LSTM and fully connected layer, and a softmax at the end for binary classification. In this model we used layers that are used in first model, along with them we used LSTM layer which is discussed below.

LSTM layer: The LSTM layer is a kind of recurrent neural network layer that is designed to process sequential data such as time series, sentences, sequences of graph embedding, etc., LSTM layer can captures long-range dependencies, reduces vanishing gradient, and versatility.

The number of layers, along with the type and the sequence in which they are used, are shown in Fig. 3(b). The hyperparameters used in this model are batch_size = 32, random_state = 42, 52, 62, 72, 82, learning_rate = 0.0001, activation_function = ReLU, and dropout = 0.1. Fig. 3 illustrates more details of each layer, the number of features, and other hyperparameters.

Developed GCN-based models, Model_1 and Model_2, were experimented with data of different epoch lengths, which are 1-sec, 4-sec, 5-sec, and 8-sec; in this work, we are presenting results of 5-sec and 8-sec epoch lengths on both the developed models because epochs lengths 1-sec and 4-sec results are not satisfactory. So, we run 4 experiments that are discussed below,

GCN_5: Model_1 experimented with 5-sec epoch data.

GCN_8: Model_1 experimented with 8-sec epoch data.

GCN_LSTM_5: Model_2 experimented with 5-sec epoch data.

GCN_LSTM_8: Model_2 experimented with 8-sec epoch data.

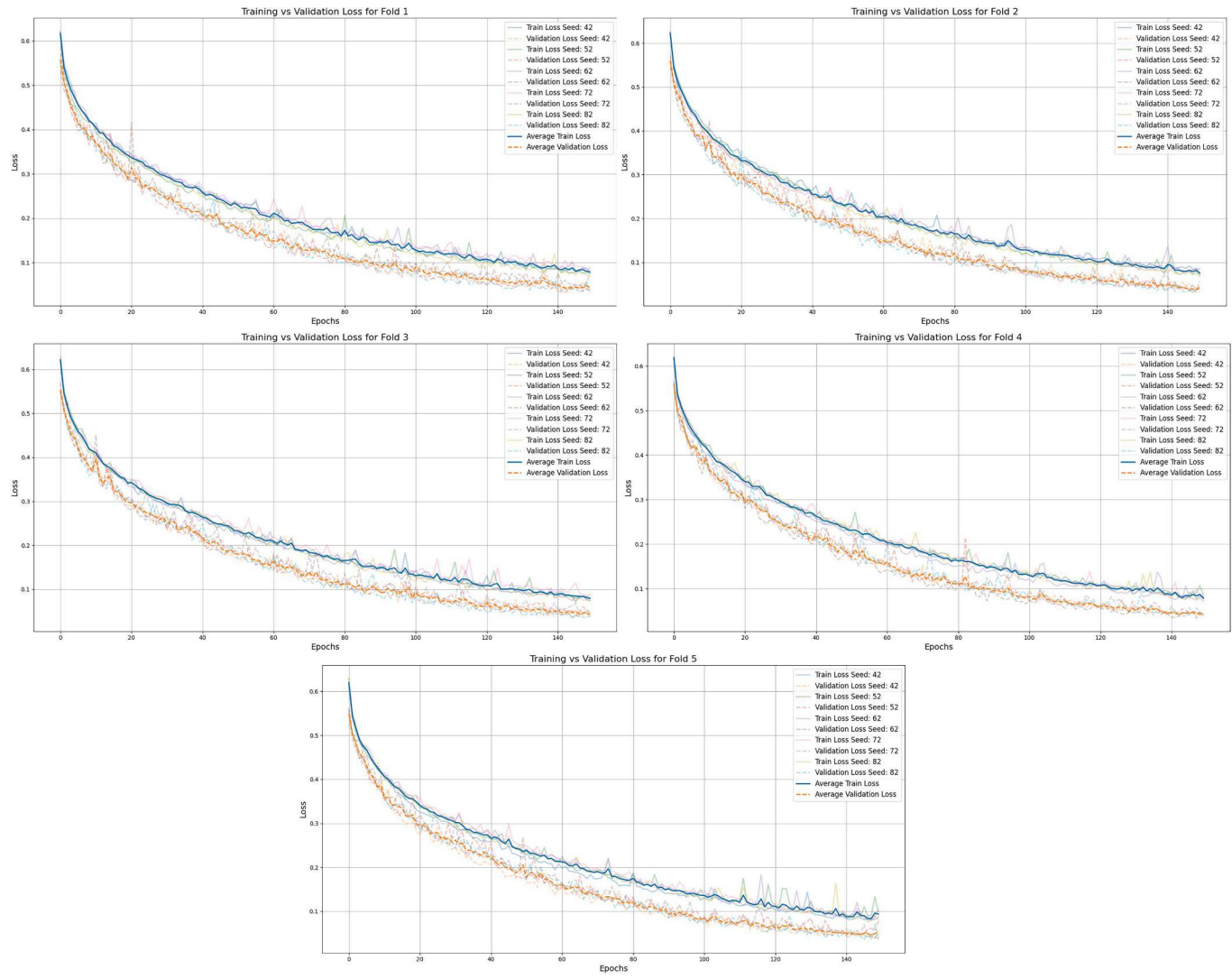


Fig. 8. The Loss function plot varying across five folds for different seeds for the GCN_LSTM_5 model.

After the models were trained, they were validated using 5-fold cross-validation. The loss was calculated for all the folds, and on each fold, we ran 150 epochs. The complete experimental flow of the developed model is shown in Fig. 4.

3.7. Hardware and software

All the experiments were conducted on an HP workstation with x64-based Intel(R) Xeon(R) w7-2475X 2.59 GHz processor, Installed RAM of 256 GB, and Windows 11 Pro for Workstations. We used Visual Studio code for developing the code and used Python programming language in the Pytorch framework to implement the developed models along with Python libraries like MNE, numpy, scipy, pandas, networkx, etc.

3.8. Evaluation metrics

To evaluate the developed models we have used eight classification performance metrics which are: accuracy, precision, recall, F1 score, sensitivity, specificity, area under the curve (AUC), and confusion matrix.

True positive (TP): If the prediction by the model is true for SZ, and the signal is also positive for SZ.

True negative (TN): If the prediction by the model is false for SZ, and the signal is also negative for SZ.

False positive (FP): If the prediction by the model is true for SZ, and the signal is also negative for SZ.

False negative (FN): If the prediction by the model is false for SZ, and the signal is also positive for SZ.

Confusion Matrix: A confusion matrix is used to evaluate the performance of the classification model, it gives the correct and incorrect predictions made by the model across different classes. Since the problem addressed in this work is a classification problem, the confusion matrix that we can get is a 2×2 matrix containing the values of true positive, false positive, true negative, and false negative as entries. The confusion matrix is shown in Fig. 5.

Accuracy: Accuracy measures the proportion of correctly predicted instances to the total number of instances, given by equation (12),

$$\text{Accuracy} = \frac{TP + TN}{TP + TN + FP + FN} \quad (12)$$

Precision: Positive predictive value (PPV) is another term for precision, it is the ratio of positively predicted values to the total number of positive values, given by equation (13)

$$\text{precision} = \frac{TP}{TP + FP} \quad (13)$$

F1 score: The F1 score is a combination of precision and recall by taking the harmonic mean of them, given by equation (14)

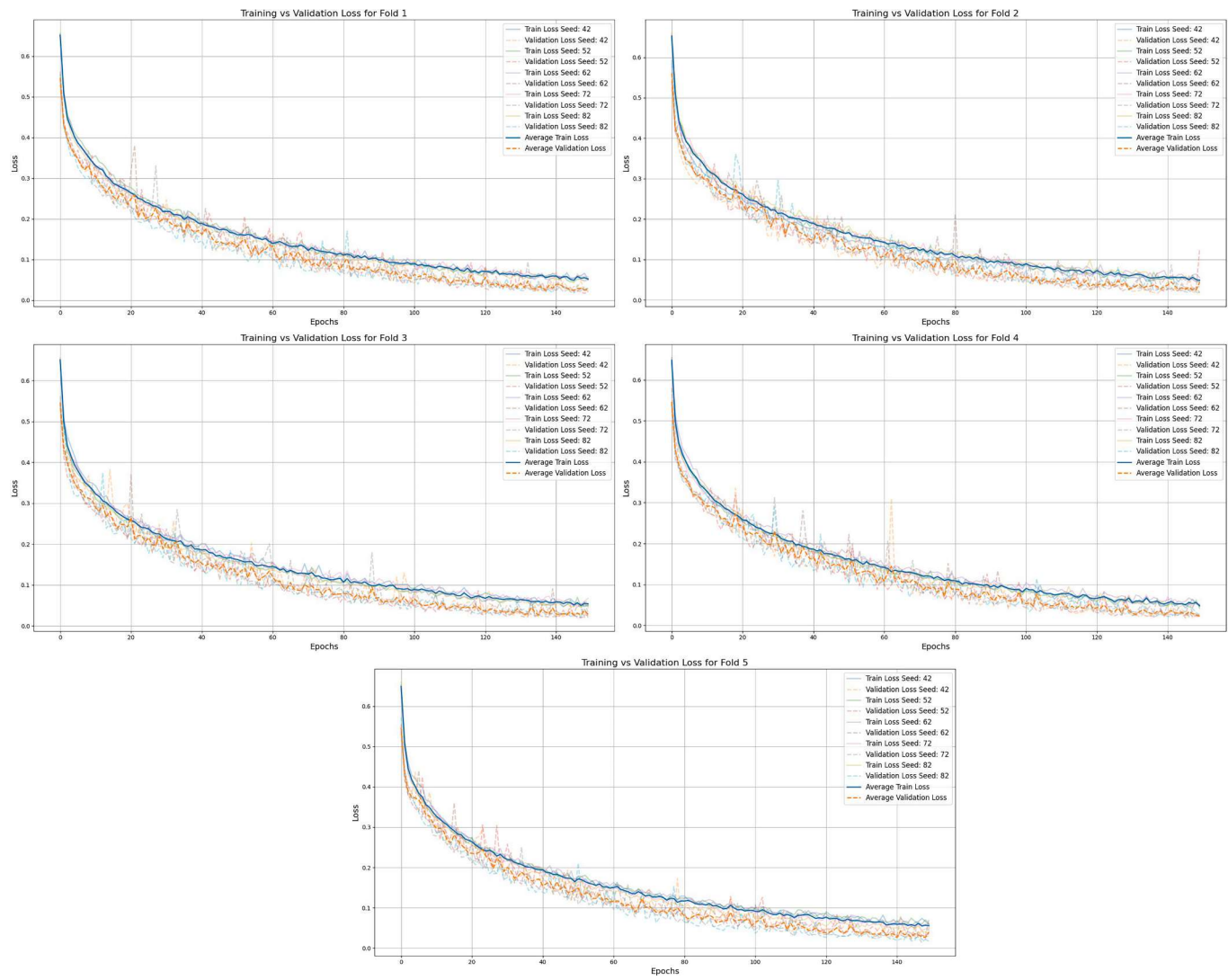


Fig. 9. The Loss function plot varying across five folds for different seeds for GCN_LSTM_8 model.

$$\text{F1 score} = 2 \frac{(\text{precision} \times \text{recall})}{(\text{precision} + \text{recall})} \quad (14)$$

Recall or Sensitivity: Recall is the ratio of true positive predictions to the total number of actual positive instances. Recall focuses on actual positive cases that the developed model correctly classified as positive, given by Eq. (15)

$$\text{Recall or Sensitivity} = \frac{TP}{TP + FN} \quad (15)$$

Specificity: Specificity also known as true negative rate, is measured by taking the proportion of actual negative instances that are correctly identified by the model. In other words, it is the accuracy of a negative prediction made by the model, given in Eq. (16)

$$\text{Specificity} = \frac{TN}{TN + FP} \quad (16)$$

Area under the curve (AUC): A metric that represents the overall performance of a binary classification model depending on the area under its ROC curve.

4. Results and analysis

We built two models based on GCN and experiments were analyzed by varying the epoch durations 5-sec and 8-sec on both models. We have

conducted the experiments several times on each model that we built by varying different hyperparameters like epoch duration, number of graph convolution layers, loss functions, and seed values, etc., and the best results in each experiment scenario i.e., GCN_5, GCN_8, GCN_LSTM_5, GCN_LSTM_8 were presented below. We divided the data into 80:20 for training and testing and used different seed values for splitting the data randomly. Seed ensures that the same data points are included each time for the train and test sets, it is important when running multiple experiments. We used five different seed values which are 42, 52, 62, 72, and 82 to run each experiment. The results of the experiments each conducted experiment are tabulated in Tables 2–5. Train-test loss of each fold for all seeds is calculated and illustrated from Figs. 6–9 and Fig. 10. shows the performance metrics of each conducted experiment. We also calculated the mean and standard deviation of all performance metrics with which we can get good insights into the conducted experiments, these are shown in the Table. 6. The average confusion matrix for developed models across seeds is shown in Fig. 11. We also compared our proposed model with the state-of-the-art models, our model performed better than SOTA models, shown in Table. 7.

4.1. GCN_5 results

GCN_5 is a combination of Model_1 with 5-sec epoch data, for this model we have achieved the best accuracy of 86.30 % achieved for seed

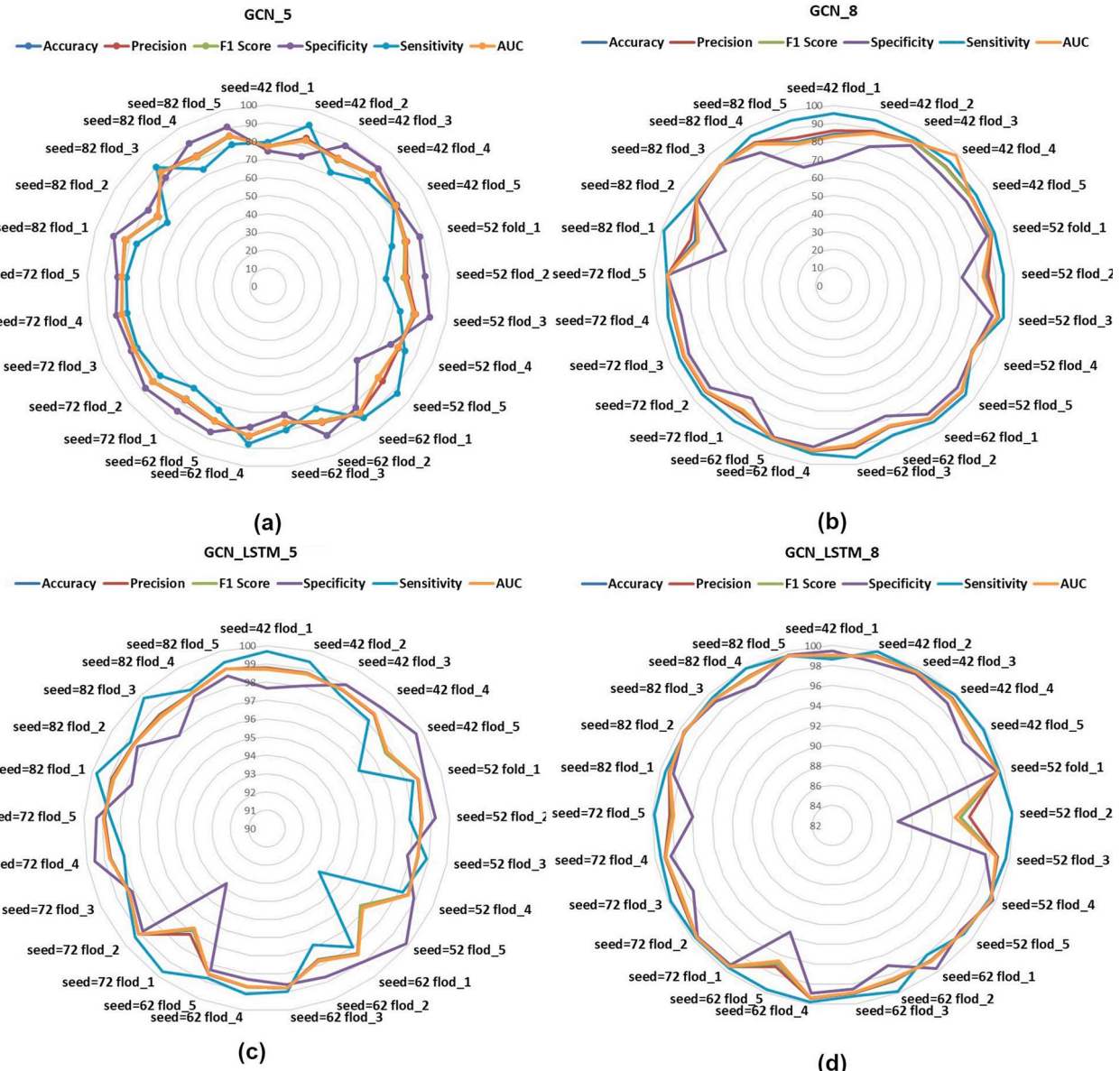


Fig. 10. Performance metrics illustration of (a) GCN_5, (b) GCN_8, (c) GCN_LSTM_5, (d) GCN_LSTM_8 models.

= 62 at fold_1 along with 86.44 % of precision, 86.21 % F1 score, 82.68 % of specificity, 89.55 % of sensitivity, and 86.12 of ACU. A similar result can also be observed for seed = 82 and fold_3. Complete details of the achieved results for the experiment GCN_5 are given in Table. 2. and Fig. 6. shows how the loss values of train and test vary across folds for different seeds.

4.2. GCN_8 results

GCN_8 is a combination of Model_1 with 8-sec epoch data, this model achieved the best accuracy of 92.67 % achieved for seed = 52 at fold_3 along with 92.88 % of precision, 92.56 % F1 score, 89.14 % of specificity, 95.56 % of sensitivity, and 92.35 of ACU. A similar result can also be observed for seed = 62 and fold_4. Complete details of the achieved results for the experiment GCN_8 are given in Table. 3. and Fig. 7. shows how the loss values of train and test vary across folds for different seeds.

4.3. GCN_LSTM_5 results

GCN_LSTM_5 is a combination of Model_2 with 5-sec epoch data, for

this model seed 72, fold_2 has achieved the best accuracy of 99.06 %, 99.07 % of precision, 99.06 % F1 score, 98.79 of specificity, 99.31 % of sensitivity, and 99.05 of ACU. The second-best accuracy is achieved for seed = 82 and fold_5. Complete details of the achieved results for the experiment GCN_LSTM_5 are given in Table. 4. and Fig. 8. shows how the loss values of train and test vary across folds for different seeds.

4.4. GCN_LSTM_8 results

GCN_LSTM_8 is a combination of Model_2 with 8-sec epoch data, for this model we have achieved the best accuracy of 99.58 % achieved for seed = 72 at fold_2, 99.58 % of precision, 99.58 % F1 score, 99.46 of specificity, 99.68 % of sensitivity, and 99.57 of ACU. The next best results can be observed for seed = 82 for fold_5. Complete details about the results of experiment GCN_LSTM_8 are given in Table. 5. and Fig. 9. shows how the loss values of train and test vary across folds for different seeds.

Table 6

Mean and standard deviation of all performance metrics of developed models GCN_5, GCN_8, GCN_LSTM_5, GCN_LSTM_8 across all folds with different seeds.

Performance Metrics		Accuracy (Mean ± SD)	Precision (Mean ± SD)	F1 Score (Mean ± SD)	Specificity (Mean ± SD)	Sensitivity (Mean ± SD)	AUC (Mean ± SD)
GCN_5	fold_1	80.38 ± 3.99	80.85 ± 3.90	80.33 ± 3.99	83.90 ± 5.79	77.22 ± 7.94	80.56 ± 3.88
	fold_2	78.43 ± 4.93	79.25 ± 4.91	78.34 ± 4.88	82.95 ± 6.47	74.38 ± 10.89	78.67 ± 4.70
	fold_3	80.96 ± 3.83	81.38 ± 3.88	80.89 ± 3.85	83.20 ± 7.49	78.96 ± 7.05	81.07 ± 3.83
	fold_4	81.95 ± 1.82	82.26 ± 1.85	81.88 ± 1.86	83.39 ± 6.65	80.66 ± 5.24	82.02 ± 1.92
	fold_5	81.45 ± 2.74	82.24 ± 2.27	81.45 ± 2.72	81.54 ± 10.36	81.41 ± 7.09	81.58 ± 2.80
GCN_8	fold_1	86.43 ± 4.58	87.81 ± 3.61	86.12 ± 5.26	77.45 ± 11.48	94.96 ± 2.30	85.80 ± 5.42
	fold_2	87.48 ± 3.60	88.03 ± 3.22	87.18 ± 3.79	81.13 ± 7.54	92.70 ± 2.48	86.91 ± 3.91
	fold_3	91.37 ± 1.08	91.60 ± 0.84	91.24 ± 1.14	88.02 ± 3.75	94.12 ± 1.95	91.07 ± 1.26
	fold_4	89.50 ± 2.80	89.66 ± 2.94	89.32 ± 2.88	86.30 ± 2.29	92.14 ± 4.37	91.02 ± 5.14
	fold_5	89.71 ± 4.12	90.15 ± 3.17	89.46 ± 4.45	85.20 ± 9.99	93.41 ± 1.22	89.30 ± 4.63
GCN_LSTM_5	fold_1	98.31 ± 0.82	98.38 ± 0.72	98.31 ± 0.83	97.44 ± 2.18	99.10 ± 0.83	98.27 ± 0.88
	fold_2	98.52 ± 0.49	98.52 ± 0.51	98.52 ± 0.49	98.63 ± 0.44	98.43 ± 1.09	98.53 ± 0.46
	fold_3	98.50 ± 0.20	98.52 ± 0.19	98.50 ± 0.20	98.09 ± 0.76	98.87 ± 0.57	98.48 ± 0.21
	fold_4	98.59 ± 0.11	98.58 ± 0.11	98.59 ± 0.11	98.80 ± 0.55	98.40 ± 0.46	98.60 ± 0.12
	fold_5	98.16 ± 1.00	98.16 ± 0.98	98.16 ± 1.00	99.16 ± 0.67	97.26 ± 2.39	98.21 ± 0.92
GCN_LSTM_8	fold_1	99.14 ± 0.28	99.12 ± 0.31	99.14 ± 0.28	99.27 ± 0.38	99.04 ± 0.68	99.15 ± 0.25
	fold_2	98.38 ± 2.02	98.59 ± 1.65	98.35 ± 2.07	96.69 ± 4.65	99.78 ± 0.23	98.23 ± 2.26
	fold_3	99.00 ± 0.35	99.05 ± 0.31	98.99 ± 0.35	98.33 ± 0.87	99.56 ± 0.21	98.94 ± 0.39
	fold_4	99.25 ± 0.24	99.28 ± 0.22	99.24 ± 0.24	98.73 ± 0.64	99.67 ± 0.28	99.20 ± 0.27
	fold_5	98.42 ± 1.00	98.55 ± 0.86	98.40 ± 1.02	97.01 ± 2.39	99.57 ± 0.31	98.29 ± 1.13

5. Discussion

In this paper, we have developed two deep-learning models for classifying EEG signals of schizophrenia from healthy control, we used a neural networks-based graph convolutional networks for this task. We have selected graph convolutional networks because they are very good at representing the connections that each EEG electrode has between them as a network. These networks will help us to understand the structural and functional behavior of the human brain. The developed model has outperformed the state-of-the-art models which can be observed from the Table 7. The model that we built has achieved near-perfect values in terms of performance. The this work we have experimented with different seed values for splitting the data randomly to make the train-test split consistent, along with it we also used the 5-fold cross-validation. Using different seeds and cross-validation will ensure the developed models are not overfitting. Asadzadeh et al. [3] achieved an accuracy of 98.75 for the subject-dependent study of emotion recognition using a graph neural network model is the best in terms of performance but our proposed model GCN_LSTM and outperformed the previous best model and other SOTA models.

5.1. Advantages and limitations of the proposed models

Model_1: The advantages of the proposed Model_1 are, that GCNs are well-suited to handle the spatial data by modeling the relationships between electrodes as graphs, and it also helps in understanding the non-Euclidean and complex brain signals. The sparse representation of GCNs can effectively handle large-scale multi-channel EEG data which reduces computational complexity. The graphs created by GCNs provide useful insights into the functional connectivity of the different brain regions. The limitations of GCNs are their performance depends on how the graph is constructed, poorly constructed graphs can lead to poorer results. GCNs are not good at studying the temporal evolution of signals, which is vital in understanding the dynamic nature of human brain activity in schizophrenia.

Model_2: The advantages of GCN-LSTM are; that it works well for both spatial and temporal information, GCN layers capture the spatial relationships between EEG channels, whereas LSTM layers model the temporal evolution of the EEG signals. Since GCN-LSTM is good at capturing temporal information, this, in turn, leads to better performance in classification tasks in terms of accuracy when compared to GCN alone. It also handles long-term dependencies very well in EEG signals, which are crucial in identifying small variations in EEG patterns

of schizophrenic patient's data. The limitations of GCN-LSTM are that it adds significant computational overhead in terms of time and is prone to overfitting because of many parameters. Hyperparameter tuning should be done very carefully because it may increase the complexity of the model, and it also requires a large amount of data for effective training.

5.2. Practical applications, real-time clinical adaptability and challenges

Decision support for clinicians: The proposed GCN-LSTM model, trained to classify schizophrenia from EEG data, can be used as a decision support tool. Clinicians can receive an on-screen alert for the probability of schizophrenia during or after EEG recording sessions. We could track how a patient's network dynamics evolve by analyzing the changes over repeated EEG sessions, potentially aiding treatment efficacy evaluation and longitudinal management.

Real-Time or Near-Real-Time Analysis: A well-optimized GCN-LSTM model along with the sufficient computing power could be adapted to process streaming EEG data in near real-time. Techniques like model pruning and quantization can further reduce compute load for on-site deployment.

Multimodal Integration: The GCN-LSTM framework can be extended beyond EEG to incorporate data from fMRI, MEG, or clinical interviews. Combining the connectivity patterns from EEG with the functional or structural MRI data can produce a more robust model.

Dataset Limitations and Biases Affecting Generalizability: Many of the EEG-based models are developed on small datasets (<100 samples) and are also data dependent. These datasets lack diversity in age, ethnicity, gender, etc., so the model may not generalize to broader populations.

Inter-Site and Inter-Device Variability: Different data recording devices have different configurations: device type (traditional/clinical or portable), variation in electrode type, number of electrodes used for recording, amplifier brands.

Selection Bias in Patient Samples: Studies often recruit from specialized psychiatric units, which might not represent the broader population. Moreover, Schizophrenia frequently co-occurs with other conditions such as, substance use disorders, mood disorders etc., A dataset that excludes or underrepresents these comorbidities may reduce the generalizability of the model to real-world patients who have these type of disorders.

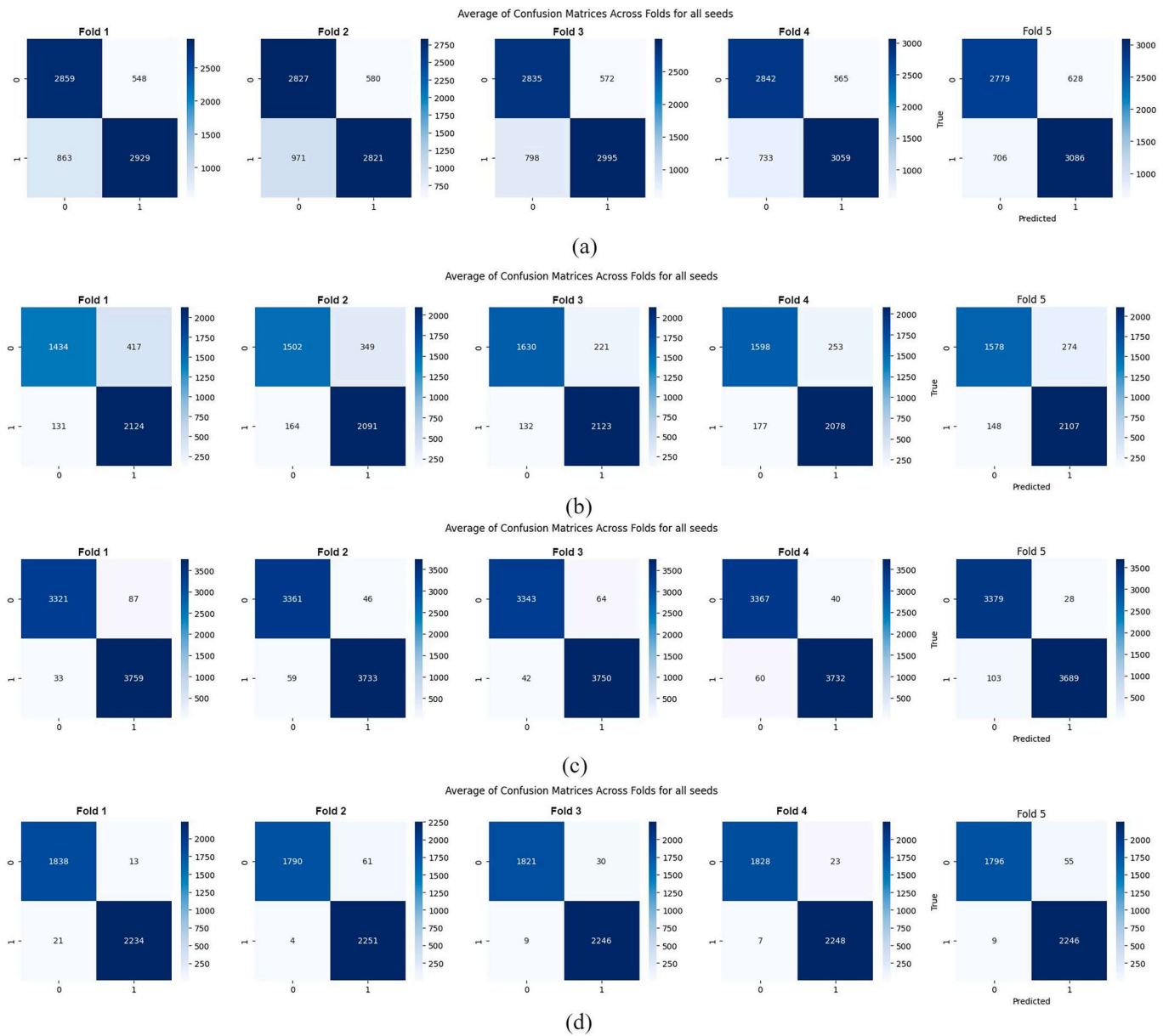


Fig. 11. Average of confusion matrix for developed models across all seeds for all folds (a) GCN_5 model, (b) GCN_8 model, (c) GCN_LSTM_5 model, (d) GCN_LSTM_8 model.

6. Conclusion and future work

In this study, we have successfully developed 10-graph convolutional layers followed by a fully connected softmax and hydride GCN-LSTM to classify EEG signals of schizophrenia from healthy control. By leveraging the graph-based structures, where electrodes represent the nodes in the graph and the connection between the nodes as edges. We pre-processed the raw EEG signal by using band-pass filtering, which removes unwanted noise and artifacts from the signal, and created the segments of 5-sec and 8-sec of duration and extracted 14 features from the EEG signal 7 from the time domain, and 7 features are from the frequency domain. The developed models were trained on graphs that were created using epoch lengths 5-sec and 8-sec. The best results were achieved with the GCN-LSTM model for the fold_4, with an Accuracy of 99.25 ± 0.24 for the GCN-LSTM model with 8-sec epoch data, also Precision of $99.28 \pm 0.22\%$, F1 score of $99.24 \pm 0.24\%$, Specificity of 98.73 ± 0.64 ; Sensitivity of 99.67 ± 0.28 and AUC of 99.20 ± 0.27 . The robustness of the developed is ensured by the use of multiple seed values

and 5-fold cross-validation, which also helps avoid overfitting.

While the current study is conducted on the Institute of Psychiatry and Neurology in Warsaw dataset for schizophrenia classification, it can be extended further in different directions by applying this framework to other neurological diseases like epilepsy, major depression disorder, Parkinson's disease, emotion recognition, etc., which have large and more diverse datasets to validate the generalizability. It can also be extended to develop a real-time model that can classify and provide easy and fast diagnosis in the clinical environment. Another direction of work is exploring other deep learning techniques like transformers, autoencoders, generative AI, explainable AI for a better understanding of the models, and graph attention networks which work well for multi-modal features. Furthermore, the research could focus on optimizing the extracted features using feature selection and dimensionality reduction methods.

Table 7

Results comparison of the proposed model with various state-of-the-art models.

Authors	Dataset	Classification Algorithm	Performance metrics (%)
Soria Bretones et al.,	Psychiatry Department of Virgen de la Luz Hospital in Cuenca (Castilla-La Mancha, Spain) (Schizophrenia)	Radial basis function (RBF) network	Acc = 93.72; Sen = 93.82; Spe = 93.38; Kap = 83.44; F1 score = 93.43
Li et al.,	Temple University Hospital (TUH) EEG corpus (Seizure)	graph-generative neural networks (GGN)	Acc = 91
P. Lin et al.,	Zenodo (EEG dataset) (Schizophrenia) 0-back dataset (Schizophrenia)	MGAT- AIR model	Acc = 90.90; F1 score = 90.90 (Zenodo) Acc = 78.57; F1-score = 80.00 (0-back dataset)
X. Lin et al.,	DEAP-Twente, DEAP-Geneva, SEED dataset	CS-Graph convolutional network	Acc = 90.74 Acc = 91.00 Acc = 90.22
Asadzadeh et al.,	The brain-computer interface research lab, University of Tabriz, Iran (Emotion Recognition)	graph neural network (GNN)	Acc = 98.75 (Subject-dependent) Acc = 97.5. (Subject-independent)
Yin et al.,	Beijing Huilongguan Hospital. Statistical (Schizophrenia)	graph neural network (EFC-GCN)	Acc = 90.01; Pre = 88.18; Rec = 94.45; F1 score = 90.85; AUC = 94.84
Li, W et al.,	MODMA SCHIZ	GCNs-FSMI	Acc = 97.18 Acc = 78.17
Shi et al.,	BCI Competition IV-2a (BCICIV-2a); High-Gamma Dataset (HGD) (motor imagery classification)	Graph convolutional networks (GCN)	Acc = 80.46; Kap = 74.00 Acc = 94.98;
Gosala et al.,	Institute of Psychiatry and Neurology Warsaw, Poland (Schizophrenia)	Decision Trees Random Forest Logistic Regression	Acc = 97.98; Sen = 98.2; Spe = 97.72; Kap = 95.94 Acc = 97.22; Sen = 97.43; Spe = 96.97; Kap = 94.41 Acc = 85.49; Sen = 87.45; Spe = 83.01; Kap = 70.55
Proposed model	Institute of Psychiatry and Neurology Warsaw, Poland (Schizophrenia)	GCN-LSTM	Acc = 99.25 ± 0.24 ; Pre = 99.28 ± 0.22 ; F1 score = 99.24 ± 0.24 ; Spe = 98.73 ± 0.64 ; Sen = 99.67 ± 0.28 ; AUC = 99.20 ± 0.27

Acc = Accuracy, Pre = Precision, Rec = Recall, Spe = Specificity, Sen = Sensitivity, AUC = Area under the curve, Kap = Kappa score.

Data availability statement

The dataset used in the study is open-source data, the link to download the dataset is given below: <https://repopd.icm.edu.pl/dataset.xhtml?persistentId=https://doi.org/10.18150/repopd.0107441>.

The main contributions of this work are as follows:

- We have developed two models: a novel 12-layer graph convolutional networks (GCNs) model, and a hybrid GCN-LSTM for classifying EEG signals of schizophrenic subjects and healthy control by constructing graphs.
- We extracted 14 different features, seven each from the time domain and frequency domain to remove the noise and artifacts, and also for dimensionality reduction. Also did the statistical analysis using independent t-test and one-way ANOVA to study the statistical significance among the extracted features.

- Cohesion analysis and phase locking values are calculated using Hilbert transformation for creating edges between the nodes (electrodes) to construct graphs.
- We experimented with epochs of 5-sec and 8-sec duration on the developed models, our proposed model outperformed all the state-of-the-art models.

CRediT authorship contribution statement

Bethany Gosala: Writing – original draft, Visualization, Validation, Project administration, Conceptualization. **Avnish Ramvinay Singh:** Methodology, Investigation, Formal analysis, Data curation. **Himanshu Tiwari:** Methodology, Investigation, Formal analysis, Data curation. **Manjari Gupta:** Writing – review & editing, Supervision, Resources, Investigation.

Declaration of competing interest

The authors declare that they have no known competing financial interests or personal relationships that could have appeared to influence the work reported in this paper.

Acknowledgment

- The author is extremely grateful to the University Grants Committee (UGC) for providing the Junior Research Fellowship (JRF) under Maulana Azad National Fellowship for Minorities (MANJRF), with the award reference number: NO.F.82-27/2019 (SA III).
- We acknowledge the Institute of Eminence (IoE) scheme at BHU for supporting us.
- We would like to thank Mr. Sushrut Patwardhan (data scientist at MOBAI, Gjovik, Norway), for his help in coding and insightful discussions on this manuscript.
- The authors extend sincere gratitude to the journal's editors and reviewers for their kind support, comments, and suggestions, which helped greatly improve the manuscript.

Data availability

I have already shared the link of data in the manuscript

References

- [1] S. Aggarwal, N. Chugh, Review of Machine Learning Techniques for EEG Based Brain Computer Interface, *Arch. Comput. Meth. Eng.* 29 (2022), <https://doi.org/10.1007/s11831-021-09684-6>.
- [2] S. Arcidiacono, May 5). *What Makes Graph Convolutional Networks Work?* Medium. (2021), <https://towardsdatascience.com/what-makes-graph-convolutional-networks-work-53bad0ce9>.
- [3] S. Asadzadeh, T.Y. Rezaii, S. Beheshti, S. Meshgini, Accurate Emotion Recognition Utilizing Extracted EEG Sources as Graph Neural Network Nodes, *Cogn. Comput.* 15 (1) (2023) 176–189, <https://doi.org/10.1007/s12559-022-10077-5>.
- [4] Bethany, G., Gosala, E., & Gupta, M. (2023). *A Deep Learning Based Model to Study the Influence of Different Brain Wave Frequencies for the Disorder of Depression* (pp. 449–458). doi: 10.1007/978-3-031-36402-0_42.
- [5] M. Chen, Z. Wei, Z. Huang, B. Ding, Y. Li, Simple and Deep Graph Convolutional Networks, in: *Proceedings of the 37th International Conference on Machine Learning, 2020*, pp. 1725–1735.
- [6] B. Gosala, P. Dindayal Kapgate, P. Jain, R. Nath Chaurasia, M. Gupta, Wavelet transforms for feature engineering in EEG data processing: An application on Schizophrenia, *Biomed. Signal Process. Control* 85 (February) (2023) 104811, <https://doi.org/10.1016/j.bspc.2023.104811>.
- [7] Hagberg, A. (n.d.). *networkx: Python package for creating and manipulating graphs and networks* (Version 3.3) [Python; OS Independent]. Retrieved June 25, 2024, from <https://networkx.org/>.
- [8] S. Hussain, I. Mubeen, N. Ullah, S.S.U.D. Shah, B.A. Khan, M. Zahoor, R. Ullah, F. A. Khan, M.A. Sultan, Modern Diagnostic Imaging Technique Applications and Risk Factors in the Medical Field: A Review, *Biomed Res. Int.* 2022 (2022) 5164970, <https://doi.org/10.1155/2022/5164970>.

- [9] M. Jafari, A. Shoeibi, M. Khodatars, S. Bagherzadeh, A. Shalbaf, D.L. García, J.M. Gorriz, U.R. Acharya, Emotion recognition in EEG signals using deep learning methods: A review, *Comput. Biol. Med.* 165 (August) (2023), <https://doi.org/10.1016/j.combiomed.2023.107450>.
- [10] W. Li, H. Wang, L. Zhuang, GCNs-FSMI: EEG recognition of mental illness based on fine-grained signal features and graph mutual information maximization, *Expert Syst. Appl.* 228 (April) (2023) 120227, <https://doi.org/10.1016/j.eswa.2023.120227>.
- [11] Z. Li, K. Hwang, K. Li, J. Wu, T. Ji, Graph-generative neural network for EEG-based epileptic seizure detection via discovery of dynamic brain functional connectivity, *Sci. Rep.* 12 (1) (2022) 1–15, <https://doi.org/10.1038/s41598-022-23656-1>.
- [12] P. Lin, G. Zhu, X. Xu, Z. Wang, X. Li, B. Li, Brain network analysis of working memory in schizophrenia based on multi graph attention network, *Brain Res.* 1831 (January) (2024) 148816, <https://doi.org/10.1016/j.brainres.2024.148816>.
- [13] X. Lin, J. Chen, W. Ma, W. Tang, Y. Wang, EEG emotion recognition using improved graph neural network with channel selection, *Comput. Methods Programs Biomed.* 231 (2023) 107380, <https://doi.org/10.1016/j.cmpb.2023.107380>.
- [14] Mental health. (n.d.). Retrieved June 22, 2024, from <https://www.who.int/news-room/fact-sheets/detail/mental-health-strengthening-our-response>.
- [15] E. Olejarczyk, W. Jernajczyk, Graph-based analysis of brain connectivity in schizophrenia, *PLoS One* 12 (11) (2017) e0188629, <https://doi.org/10.1371/journal.pone.0188629>.
- [16] K. Rasheed, A. Qayyum, J. Qadir, S. Sivathamboo, P. Kwan, L. Kuhlmann, T. O'Brien, A. Razi, Machine Learning for Predicting Epileptic Seizures Using EEG Signals: A Review, *IEEE Rev. Biomed. Eng.* 14 (c) (2021) 139–155, <https://doi.org/10.1109/RBME.2020.3008792>.
- [17] Schizophrenia. (n.d.). Retrieved June 22, 2024, from <https://www.who.int/news-room/fact-sheets/detail/schizophrenia>.
- [18] S. Secinaro, D. Calandra, A. Secinaro, V. Muthurangu, P. Biancone, The role of artificial intelligence in healthcare: A structured literature review, *BMC Med. Inf. Decis. Making* 21 (1) (2021) 125, <https://doi.org/10.1186/s12911-021-01488-9>.
- [19] J. Shi, J. Tang, Z. Lu, R. Zhang, J. Yang, Q. Guo, D. Zhang, A brain topography graph embedded convolutional neural network for EEG-based motor imagery classification, *Biomed. Signal Process. Control* 95 (PB) (2024) 106401, <https://doi.org/10.1016/j.bspc.2024.106401>.
- [20] A. Shoeibi, M. Khodatars, M. Jafari, N. Ghassemi, P. Moridian, R. Alizadehsani, S. H. Ling, A. Khosravi, H. Alinejad-Rokny, H.K. Lam, M. Fuller-Tyszkiewicz, U. R. Acharya, D. Anderson, Y. Zhang, J.M. Gorriz, Diagnosis of brain diseases in fusion of neuroimaging modalities using deep learning: A review, *Inf. Fusion* 93 (2023) 85–117, <https://doi.org/10.1016/j.inffus.2022.12.010>.
- [21] C. Soria Bretones, C. Roncerio Parra, J. Cascón, A.L. Borja, J. Mateo Sotos, Automatic identification of schizophrenia employing EEG records analyzed with deep learning algorithms, *Schizophr. Res.* 261 (July) (2023) 36–46, <https://doi.org/10.1016/j.schres.2023.09.010>.
- [22] Wu, Z., Pan, S., Chen, F., Long, G., Zhang, C., & Yu, P. S. (2021). A Comprehensive Survey on Graph Neural Networks. *IEEE Transactions on Neural Networks and Learning Systems*, 32(1), 4–24. IEEE Transactions on Neural Networks and Learning Systems. doi: 10.1109/TNNLS.2020.2978386.
- [23] X. Yao, X. Wang, S.-H. Wang, Y.-D. Zhang, A comprehensive survey on convolutional neural network in medical image analysis, *Multimed. Tools Appl.* 81 (29) (2022) 41361–41405, <https://doi.org/10.1007/s11042-020-09634-7>.
- [24] G. Yin, Y. Chang, Y. Zhao, C. Liu, M. Yin, Y. Fu, D. Shi, L. Wang, L. Jin, J. Huang, D. Li, Y. Niu, B. Wang, S. Tan, Automatic recognition of schizophrenia from brain-network features using graph convolutional neural network, *Asian J. Psychiatr.* 87 (April) (2023) 103687, <https://doi.org/10.1016/j.ajp.2023.103687>.
- [25] Yu, H., Lei, X., Song, Z., Liu, C., & Wang, J. (2020). Supervised Network-Based Fuzzy Learning of EEG Signals for Alzheimer's Disease Identification. *IEEE Transactions on Fuzzy Systems*, 28(1), 60–71. IEEE Transactions on Fuzzy Systems. doi: 10.1109/TFUZZ.2019.2903753.
- [26] Yu, H., Li, F., Liu, J., Liu, D., Guo, H., Wang, J., & Li, G. (2024). Evaluation of Acupuncture Efficacy in Modulating Brain Activity With Periodic-Aperiodic EEG Measurements. *IEEE Transactions on Neural Systems and Rehabilitation Engineering*, 32, 2450–2459. IEEE Transactions on Neural Systems and Rehabilitation Engineering. doi: 10.1109/TNSRE.2024.3421648.
- [27] Yu, H., Li, X., Lei, X., & Wang, J. (2019). Modulation Effect of Acupuncture on Functional Brain Networks and Classification of Its Manipulation With EEG Signals. *IEEE Transactions on Neural Systems and Rehabilitation Engineering*, 27(10), 1973–1984. IEEE Transactions on Neural Systems and Rehabilitation Engineering. doi: 10.1109/TNSRE.2019.2939655.
- [28] Yu, H., Wu, X., Cai, L., Deng, B., & Wang, J. (2018). Modulation of Spectral Power and Functional Connectivity in Human Brain by Acupuncture Stimulation. *IEEE Transactions on Neural Systems and Rehabilitation Engineering*, 26(5), 977–986. IEEE Transactions on Neural Systems and Rehabilitation Engineering. doi: 10.1109/TNSRE.2018.2828143.